Icarus 232 (2014) 1–12

Contents lists available at ScienceDirect

Icarus

journal homepage: www.elsevier.com/locate/icarus

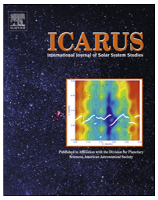

Transverse motion of fragmenting faint meteors observed with the Canadian Automated Meteor Observatory

E. Stokan [*], M.D. Campbell-Brown

Department of Physics and Astronomy, University of Western Ontario, London, Ontario N6A 3K7, Canada

ARTICLE INFO

Article history:
Received 8 November 2013
Revised 21 December 2013
Accepted 1 January 2014
Available online 9 January 2014

Keywords:
Meteors
Interplanetary dust
Image processing

ABSTRACT

Nine fragmenting, faint meteors (peak magnitude $\sim +1$, mass $< 10^{-4}$ kg) were observed with the Canadian Automated Meteor Observatory (CAMO). Fragments for eight of the nine meteors exhibited significant transverse motion, perpendicular to the meteor velocity. Transverse speeds of the order 100 m s^{-1} were observed, while models of aerodynamic loading predict speeds of the order 0.5 m s^{-1}. Acceleration of the fragments in the transverse direction was negligible. Alternate methods of fragmentation, namely rotation and electrostatic charge accumulation, were examined through basic models to explain the observed transverse speeds. Meteoroid strengths of the order 10^6 Pa were derived, matching observed strengths of larger, brighter meteors.

1. Introduction

As meteoroids enter the atmosphere, they begin to ablate and emit light. The resulting light curve, plotting intensity as a function of height, serves as an important constraint for meteoroid ablation models. These models provide information about ablation processes, meteoroid composition, and atmospheric chemistry (Hawkes and Jones, 1975; Boyd, 2000; Campbell-Brown and Koschny, 2004). Meteoroid fragmentation is also an important process to characterise, as it biases radar observations (Campbell-Brown and Jones, 2003; Baggaley and Grant, 2004) and can provide insight into meteoroid strength and composition (Ceplecha et al., 1998; Borovička and Kalenda, 2003).

Fragmentation can occur on a scale ranging from gross (or macroscopic) fragmentation, where the meteoroid splits into a small number of discernible pieces that separate, to continuous (or microscopic) fragmentation, where the fragments are small and numerous enough to not be distinguishable. Gross fragmentation typically occurs for bright meteors such as Peekskill (Brown et al., 1994), or more recently, Chelyabinsk (Borovička et al., 2013), and is observed directly in video and photographic records, or indirectly as sharp spikes or flares in the meteor light curve. Conversely, continuous fragmentation is expected to be more common for fainter, less massive objects, and has been modelled as an explanation for the size and height-dependence of the faint meteor initial ion trail (Hawkes and Jones, 1978; Campbell-Brown and Jones, 2003).

Observing gross fragmentation in faint meteors with video is challenging due to the requirements of high brightness sensitivity and fine spatial resolution, both needed to discern the individual, faint fragments. Faint meteors are often observed with backscatter radar rather than video, which is more sensitive to continuous fragmentation (and the associated widening of the ion trail detected by the radar) than gross fragmentation. This may explain why gross fragmentation is observed more commonly in brighter meteors. Possible faint meteor gross fragmentation was observed with radar by Elford and Campbell (2001) as oscillations in the meteor head echo amplitude.

Alternately, fragmentation in faint and bright meteors may be the same physical process, but at different size scales. Jacchia (1955) notes that ablation continuously detaches the grains that comprise a meteoroid. For a small meteoroid producing a faint meteor, these grains are of comparable size to the meteoroid. This is not the case for a brighter, more massive body, which is expected to be much larger than the size of its constituent grains. As a result, smaller meteoroids will appear to continuously fragment, while the continuous fragmentation of larger bodies will not be perceptible. Instead, macroscopic fragmentation related to the inhomogeneity of a larger body would be observed at later stages of the meteoroid ablation.

The principal mechanism for the gross fragmentation of large objects is usually taken to be aerodynamic loading (Passey and Melosh, 1980; Artemieva and Shuvalov, 2001). Determining the atmospheric density at the height of fragmentation and calculating

---

[*] Corresponding author. Address: University of Western Ontario, 1151 Richmond Street, London, Ontario N6A 3K7, Canada.

E-mail address: estokan@uwo.ca (E. Stokan).

0019-1035/$ - see front matter © 2014 Elsevier Inc. All rights reserved.
http://dx.doi.org/10.1016/j.icarus.2014.01.002

a cross-sectional area for the meteoroid (given a shape, mass and assumed density) gives the aerodynamic pressure on the body at the point of fragmentation, which is taken to be equal to the strength of the meteoroid. Strength values of 10^6 and 10^7 Pa have been measured for the Benešov and Sikhote-Alin meteorites, respectively (Artemieva and Shuvalov, 2001). Borovička and Kalenda (2003) calculated a strength of 5×10^6 Pa based on the height of fragmentation for the Morávka meteoroid. Passey and Melosh (1980) suggested strengths between 10^5 and 10^8 Pa for bright meteors that yielded meteorites. Similarly, Popova et al. (2011) determined strengths between 10^5 and 10^7 Pa in a review of 13 fragmenting meteoroids that produced meteorites.

For fainter objects, macroscopic fragmentation is less understood as the process occurs at relatively large heights ($h \geqslant 80$ km) where the atmosphere is rarefied. Trigo-Rodríguez and Llorca (2006, 2007) obtained strengths of the order 10^4 Pa for a number of shower meteors with cometary parent bodies. These were determined by assuming that flares in the light curve represented fragmentation and obtaining the corresponding aerodynamic pressure at those heights. Similarly, Borovička et al. (2007) obtained a strength of 5×10^3 Pa for a Draconid meteor, but suggested that meteoroid heating may have been more significant in causing fragmentation than aerodynamic pressure at a height of 100 km. In any case, bright meteors appear stronger than faint meteors, though it should be noted that many of the faint, high-altitude meteors studied were from cometary parent bodies.

Several alternate mechanisms have been proposed for fragmentation associated with faint meteors, such as rotation (Hawkes and Jones, 1978), catastrophic charging (Spurný and Ceplecha, 2008), or explosive devolatilization (Kramer, 1968; Stoch, 1991). Evaluation and refinement of these models has been hindered by few direct, high-resolution observations of gross fragmentation in faint meteors. Similarly, the transverse spreading of the fragments from faint meteors is poorly understood. As aerodynamic drag is proportional to the cross-section area of the object, fragments with different masses are expected to drift apart in the direction of travel, forming a meteor trail. At lower heights, around 50 km, flowfield interaction accounts for dispersion of fragments perpendicular to the meteor trail (Artemieva and Shuvalov, 2001). This provides an explanation for deeply-penetrating meteoroids. Conversely, for faint meteors at higher altitudes characterised by free molecular flow, there is negligible flowfield interaction as atmospheric particles collide directly with the meteoroid, with ablated meteor vapour providing negligible shielding (Campbell-Brown and Koschny, 2004).

The Canadian Automated Meteor Observatory (CAMO) is a two-station, high-resolution, image-intensified video system that has captured approximately 3000 meteors operating from August 2010 and 2013. Examining the events for fragmentation is an ongoing process, but 1800 have been inspected so far, and 311 were observed to have gross fragmented, showing at least two distinct fragments. Of those meteors, 32 were observed to show possible transverse (perpendicular to meteor trail) motion for the fragments. CAMO is able to provide high-resolution data to constrain models of gross fragmentation in faint meteors, and has already been used to provide new observations of faint meteor trails (Stokan et al., 2013) and test current dustball ablation models (Campbell-Brown et al., 2013). The goals of this study are: to select a small number (9) of the highest-quality observations of faint meteor gross fragmentation, with fragments showing transverse motion; to characterise the fragment transverse motion (determine the speed of the motion and whether the fragments are accelerating, extrapolate a height of fragmentation); and, to apply basic iterations of fragmentation models to suggest what caused the fragmentation and transverse spreading.

2. Instruments and analysis

2.1. The Canadian Automated Meteor Observatory

CAMO is an image-intensified, automated video system, comprised of two stations located in southern Ontario, Canada. The stations are separated by a baseline of 45 km. At each station, a camera with a wide, 28° field of view (25 mm *f*/0.85 lens) automatically detects meteors and provides tracking information for a complementary, narrow-field camera that follows the meteor in flight. The narrow-field system uses two mirror-mounted galvanometers to guide light from the meteor into a ZenithStar 80 mm *f*/6.8 telescope. This gives a 1.5° field of view for high spatial resolution observations of the meteor.

The wide- and narrow-field systems both use Imperx IPX-VGA120L cameras with 640 × 480 pixel resolution at 12-bits per pixel to minimise image saturation. Both systems are lens-coupled to third-generation ITT NiteCam 380i image intensifiers with nominal sensitivity between 500 and 800 nm. The limiting detection magnitude for meteors observed with CAMO is approximately +5, giving an approximate mass sensitivity limit of 10^{-6} kg. The wide-field system operates at 80 frames per second, while the narrow-field system operates at 110 frames per second. The galvanometers tracking the meteor for the narrow-field system update positions at 2000 Hz to ensure smooth tracking based on a linear fit prepared in real-time using wide-field data. This is an evolution of the AIM-IT system developed by Gural et al. (2004). All narrow- and wide-field cameras are synchronised by GPS clock to allow for direct comparison of observations from all cameras. In practise, the lag between systems is less than one narrow-field frame.

The detection, tracking, and capture of the meteors with both cameras is completely automated, allowing for a large number of observations per night. Additional details regarding the system are available in Weryk et al. (2013).

For one of the nine meteors studied, wide-field observations were obtained with the CAMO influx system. The influx system is comprised of two high-resolution wide-field cameras (Cooke PCO.1600 with a 50 mm *f*/0.95 lens; one camera at each station) and is used to measure meteoroid orbits with high precision (Musci et al., 2012). The influx cameras also use ITT NiteCam intensifiers and have a similar spectral response as the narrow- and wide-field systems, though with a limiting meteor magnitude of +6.5. The system has a 20° field of view, capturing videos at 1600 × 1200 resolution, 20 frames per second, with 14-bits per pixel. A delay of 0.06 ms was measured between the influx system and the narrow- and wide-field systems and compensated for in all calculations.

2.2. Wide-field reductions

Data from the double-station wide-field cameras were used to determine the trajectory and light curve for each meteor. The software package METAL (Weryk and Brown, 2012) allows the position of the meteor to be selected in each frame of the wide-field video. An astrometric and photometric plate is created for each station by selecting stars in the field of view, calibrating their pixel position and instrumental magnitude (logarithm of the summed brightness of the star) with catalogue position and magnitude, respectively. The trajectory solver MILIG (Borovička, 1990), integrated into METAL, calculates the trajectory of the meteor using the position of the meteor in each frame of the videos from both stations. The instrumental, apparent magnitude of the meteor in each frame is converted to an *R*-band magnitude with the photometric plate, and then converted to an absolute magnitude using the computed range to the meteor at each frame time. Astrometry and photome-